Genetics of shoulder girdle formation: roles of Tbx15 and aristaless-like genes

Sanne Kuijper[1], Annemiek Beverdam[1,*], Carla Kroon[1], Antje Brouwer[1], Sophie Candille[2], Gregory Barsh[2] and Frits Meijlink[1,†]

[1]Hubrecht Laboratory, The Netherlands Institute for Developmental Biology, Uppsalalaan 8, 3584CT Utrecht, The Netherlands
[2]Departments of Genetics and Pediatrics, Stanford University School of Medicine, Stanford, CA, USA
*Present address: Institute for Molecular Bioscience, The University of Queensland, Brisbane, Queensland, Australia
†Author for correspondence (e-mail: frits@niob.knaw.nl)

Accepted 2 February 2005

Development 132, 1601-1610
Published by The Company of Biologists 2005
doi:10.1242/dev.01735

Summary

The diverse cellular contributions to the skeletal elements of the vertebrate shoulder and pelvic girdles during embryonic development complicate the study of their patterning. Research in avian embryos has recently clarified part of the embryological basis of shoulder formation. Although dermomyotomal cells provide the progenitors of the scapular blade, local signals appear to have an essential guiding role in this process. These signals differ from those that are known to pattern the more distal appendicular skeleton. We have studied the impact of *Tbx15*, *Gli3*, *Alx4* and related genes on formation of the skeletal elements of the mouse shoulder and pelvic girdles. We observed severe reduction of the scapula in double and triple mutants of these genes. Analyses of a range of complex genotypes revealed aspects of their genetic relationship, as well as functions that had been previously masked due to functional redundancy. *Tbx15* and *Gli3* appear to have synergistic functions in formation of the scapular blade. Scapular truncation in triple mutants of *Tbx15*, *Alx4* and *Cart1* indicates essential functions for *Alx4* and *Cart1* in the anterior part of the scapula, as opposed to *Gli3* function being linked to the posterior part. Especially in *Alx4/Cart1* mutants, the expression of markers such as *Pax1*, *Pax3* and *Scleraxis* is altered prior to stages when anatomical aberrations are visible in the shoulder region. This suggests a disorganization of the proximal limb bud and adjacent flank mesoderm, and is likely to reflect the disruption of a mechanism providing positional cues to guide progenitor cells to their destination in the pectoral girdle.

Key words: Aristaless-like genes, Gli3, Mouse mutants, Pax genes, Scapula, Skeletogenesis, Tbx15

Introduction

Although insight into the essentials of limb patterning has been rapidly increasing in recent years (Niswander, 2003), the development of the shoulder and pelvic girdle has remained more elusive. The much-studied signaling centers that are responsible for patterning of the limb bud often have little or no impact on the formation of shoulder or pelvis, and many of the classical or artificially made mutants that show an affected limb phenotype have normal skeletal elements of the girdles. However, studies involving the manipulation of chick embryos have greatly advanced our understanding of the embryology of shoulder formation. For instance, Huang and coworkers (Huang et al., 2000) identified a set of eight dermomyotomes as the origin of the scapular blade, whereas, by contrast, the scapular head derives from the somatopleure. It also became clear that signals from the surface ectoderm provide essential instructive signals (Ehehalt et al., 2004).

Relatively few mutants display disturbed pectoral girdle development, and even less show total absence of one or more elements. Pellegrini et al. reported a total lack of the scapula blade and ilium in *Emx2* mutants, whereas the remainder of the limb remained mostly intact (Pellegrini et al., 2001). Despite this striking observation it was recently concluded from detailed functional analyses in chick that *Emx2* is not sufficient for inducing shoulder structures (Pröls et al., 2004). These authors described its role as providing positional signals to cells fated to contribute to the skeletal elements of the shoulder. Loss of function of the forelimb-specific gene *Tbx5* can lead to total absence of the limb, including the scapula (Ahn et al., 2002; Ng et al., 2002; Rallis et al., 2003; Takeuchi et al., 2003). As this phenotype resulted from an experimental design where loss of function was restricted to limb bud mesoderm, it was suggested that a disturbed recruitment of cells caused the absence of the scapula (Rallis et al., 2003). Both of these examples underscore the notion that – even after the correct laying down of progenitor structures – disruption of positional cues may suffice to totally ablate skeletal elements of the shoulder.

Genes functionally linked to shoulder formation by less dramatic phenotypes in loss-of-function mutants include the Paired box gene *Pax1*, which is allelic with the classical *undulated* mutant (Balling et al., 1988), *Hoxa5* (Aubin et al., 1998), the mutant of which has a reduced acromion, *Pbx1*, the mutant of which has a reduced scapular blade (Selleri et al., 2001), and the Polycomb homolog M33, the mutant of which

has a hole in the scapular blade (Core et al., 1997). Such a scapular foramen may also be present in embryos homozygous for the *Extra toes* (*Xt*) mutation, which is allelic with *Gli3* (Hui and Joyner, 1993; Johnson, 1967), and with near-complete penetrance in *de* (*droopy ear*) mutants (Curry, 1959). We recently demonstrated that *de* is allelic with *Tbx15* (Candille et al., 2004). Very recently, and after the first submission of the present manuscript, a very thorough description of the skeletal phenotype of *de* was published (Singh et al., 2005).

Here we show that the aristaless-related genes *Alx4* and *Cart1* – previously linked to functions in limb and craniofacial development (Qu et al., 1999; Beverdam et al., 2001; Meijlink et al., 2003) – are implicated in shoulder girdle development, a role that was previously concealed by the redundancy of their functions. We investigated in more detail the phenotype of *Tbx15* mutants, exploring its genetic interactions with *Gli3*, *Alx4* and *Cart1*. In spite of the similar scapular phenotypes of *Gli3* and *Tbx15* mutants, the very strong defect seen in *Tbx15*/*Gli3* embryos suggests a synergistic functional relationship between these two genes. By contrast, the phenotype seen in *Tbx15*/*Alx4*/*Cart1* triple mutants appears to be a mere addition of phenotypes seen in the single mutants. This suggests complementary functions, and a connection to parallel processes of *Gli3* on the one hand, and to *Alx4* and *Cart1* on the other. Expression of several genes that represent markers for the different cell types contributing to the shoulder elements, including the chondrocyte marker *Pax1*, were affected in *Gli3*, *Tbx15* and *Alx4*/*Cart1* mutants. Strikingly, in *Alx4*/*Cart1* mutants *Pax1* expression was ventrally shifted. In addition, the myogenic marker *Pax3*, whose expression domain does not overlap with that of *Alx4* and *Cart1*, was abnormally expressed in *Alx4*/*Cart1* but not *Tbx15* or *Gli3* mutants. These results appear to point to a disruption of local signals, implying that in these mutants, ectopic positional cues are causative of the skeletal defects.

Materials and methods

Mutant mice lines

Tbx15 (de^H), *Alx4* (Lst^J) and *Gli3* (Xt^J) mutant mice were originally obtained from the Jackson Laboratory (Bar Harbor, Maine, USA). *Alx3* mutant mice were generated in our laboratory (Beverdam et al., 2001). *Cart1* mutant mice were obtained from B. de Crombrugghe, Houston, Texas (Zhao et al., 1996). All experiments were conducted under the approval of the animal care committee of the KNAW (Netherlands Royal Academy of Arts and Sciences). Genotyping was done by PCR on ear cuts or yolk sac DNA. *Tbx15*, *Alx3*, *Alx4*, *Cart1 and Gli3* embryos and mice were genotyped as described previously (Candille et al., 2004; Beverdam et al., 2001; Te Welscher et al., 2002).

Mice were bred in a mixed genetic background. Most of the phenotypes observed were influenced by this variable background, but this variability was minor when compared with the morphological consequences seen in comparisons between single and double mutants. Moreover, conclusions on genotype-phenotype relationships were always based on, or consistent with, comparisons of embryos within one litter, in which the contribution of alleles of unlinked modifier genes should be essentially identical.

Nomenclature and definitions

For the sake of simplicity, throughout this paper we refer to de^H mutants as '*Tbx15* mutants', to Lst^J mutants as '*Alx4* mutants', and to Xt^J mutants as '*Gli3* mutants'. The terms anterior and posterior with respect to the scapular blade may seem ambiguous, but refer in this paper to *supraspinatus fossa* and *infraspinatus fossa*, respectively.

Analysis of embryos and newborn mice

Bone and cartilage staining was done essentially as described (Beverdam et al., 2001). Whole-mount in situ hybridization using digoxigenin-labeled RNA probes was performed as described (Leussink et al., 1995; Ten Berge et al., 1998a), and in situ hybridization on sections was essentially as described (Gregorieff et al., 2004). Probes used included *Alx4*, *Gli3* (Te Welscher et al., 2002), *Pax1* (Balling et al., 1988), *Pax3* (Goulding et al., 1991), *Emx2* (Simeone et al., 1992), *Scleraxis* (Cserjesi et al., 1995) and *Tbx15*. To prepare a *Tbx15* in situ probe, a 762-bp fragment corresponding to part of the last exon was PCR-amplified from genomic DNA and subcloned in a pGEM-T vector (Promega, Madison, WI). Primers used were 5′-CCCTTCAACTAATAATCAGC-3′ (forward) and 5′-GAAGCCAAGTCCAGGTGTAGC-3′ (reverse).

Proliferating cells were detected using rabbit anti-phospho-histone H3 (Upstate, Charlottesville, VA, USA), according to manufacturer's protocol. Cells in equal areas of controls and mutants were counted and the average number compared. Apoptotic cells were detected using rabbit anti-cleaved Caspase-3 (Cell Signaling, Beverly, MA, USA), according to manufacturer's protocol. For Nile Blue (Sigma) staining, embryos were dissected and directly stained in 2 ml of DMEM culture medium containing 2 μl of 1.5% Nile Blue at 37°C, then washed with PBS for several hours and photographed.

Results

Skeletal malformations in *Tbx15* mutants

We recently reported that a 216-kb deletion in the *Tbx15* gene causes the *droopy ear* (*de*) mutation, and explored *Tbx15* function in dorsoventral patterning of pigmentation (Candille et al., 2004). Here, we have studied aspects of the skeletal phenotype of this mutant. Figure 1 shows characteristic features of *Tbx15* expression that may be relevant to the skeletal abnormalities seen in *de* mutants (Agulnik et al., 1998; Candille et al., 2004; Singh et al., 2005); expression of a zebrafish orthologue was also reported (Begemann et al., 2002). Expression was detected in mesenchyme of the limb buds from embryonic day (E) 9.5 (not shown) and, at E10.5, was seen to be highest in a medial-proximal domain (Fig. 1A). At later stages it appears to demarcate the developing zeugopodal elements (shown for the hind limbs at E11.5; Fig. 1B). In the head, it is expressed in lateral mesenchyme near the surface ectoderm (Fig. 1K). In the mandibular arch, it is expressed in two bilateral spots of mesenchyme adjacent to the ectoderm at the caudal side of the arch. *Tbx15* is also expressed in the notochord, but unlike the archetypical T-box gene *Brachyury*, expression is restricted to the part of the notochord anterior from the caudal hindbrain. Expression extends from the notochord into the surrounding cranial mesenchyme (Fig. 1J,L).

To study skeletal abnormalities, we compared Alcian Blue/Alizarin Red stainings of newborn wild-type and $Tbx15^{-/-}$ mice; heterozygous mice were indistinguishable from wild types (not shown). Figure 2A-F shows abnormalities in the skull and pectoral girdle of newborn $Tbx15^{-/-}$ mice. The defects found in the cervical vertebrae, notably the atlas and axis, are intriguing (Fig. 2D). Curry reported that the dens of the axis was displaced to the atlas, resulting in a situation reminiscent of that in more primitive vertebrates (Curry, 1959). In normal development, the atlas (1st vertebra) loses its vertebral body to

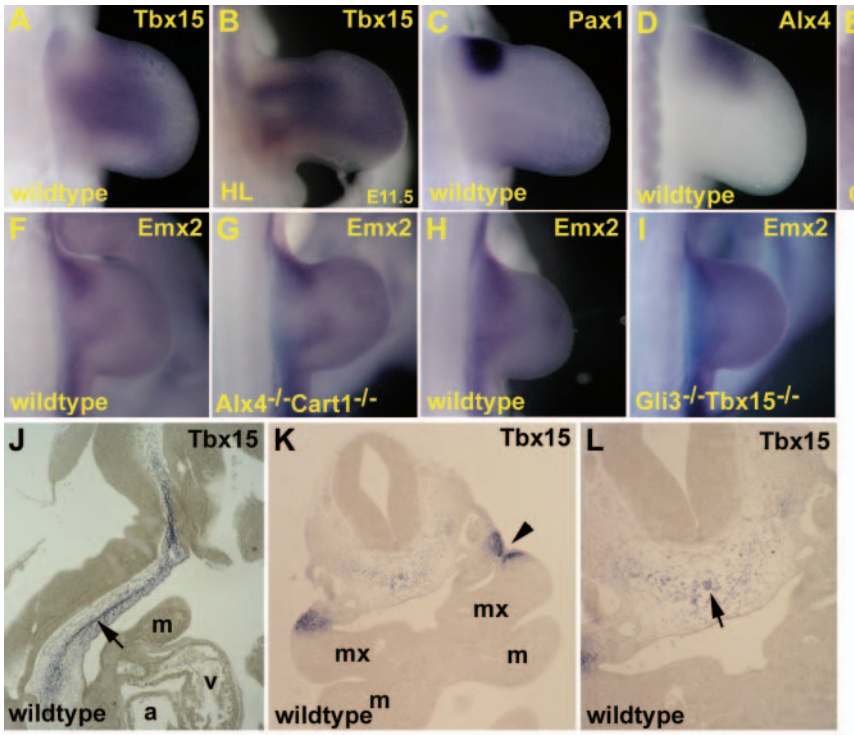

Fig. 1. Expression of *Tbx15* at E10.5. (A) Expression of *Tbx15* in wild-type forelimb bud at E10.5. (B) Expression of *Tbx15* in hindlimb bud at E11.5. (C) *Pax1* expression in wild-type forelimb bud at E10.5. Note that the expression of *Pax1* in the shoulder-forming region is complementary with that of *Tbx15*. (D,E) *Alx4* expression in wild-type (D) and $Gli3^{-/-}$ (E) forelimb buds at E10.5. In $Gli3^{-/-}$ limb buds, *Alx4* expression is downregulated in the distal part of its normal expression domain. (F-I) Expression of *Emx2* in wild-type (F,H), $Alx4^{-/-}/Cart1^{-/-}$ (G) and $Gli3^{-/-}/Tbx15^{-/-}$ (I) forelimb buds at E10.5. (J) *Tbx15* in situ hybridization on a wild-type sagittal section at E10.5. Black arrow indicates expression in notochord and surrounding mesenchyme. (K,L) *Tbx15* in situ hybridization on wild-type transverse sections at E10.5. (K) Black arrowhead shows expression of *Tbx15* in lateral cranial mesenchyme. (L) Higher magnification of section shown in K showing expression of *Tbx15* in notochord (black arrow) and surrounding mesenchyme. a, atrium; m, mandibular component; mx, maxillary component of first branchial arch; v, ventricle.

the axis (2nd vertebra), where it forms the dens. In the *Tbx15* mutants, these distinctive traits are partly lost: the dens of axis is reduced (arrowhead in Fig. 2D) and ectopic cartilage, including at this stage a tiny ossification centre, is present at a corresponding position (arrow) in the mutant atlas. It seems plausible that this aspect of the phenotype somehow relates to *Tbx15* expression in notochord and surrounding mesenchyme (Fig. 1J,L), particularly as Curry had already noted a 'double thickening of the notochord in the dens' in *Tbx15* mutant embryos at a stage (E16) when the notochord has 'normally almost disappeared' (Curry, 1959). The neural arches of $Tbx15^{-/-}$ skeletons exhibit various abnormalities, including an axis with widened arches along the anteroposterior direction (not shown). Comparison of the cranial base of wild-type versus $Tbx15^{-/-}$ mice (Fig. 2E,F) demonstrates that the $Tbx15^{-/-}$ skull is shorter and narrower than that of wild-type mice. This presumably causes, or contributes to, the abnormal position of the ears. We did not observe abnormal fusion of the supraoccipital and exo-occipital bones, as described by Curry. *Tbx15* mutants also have a comparatively narrow basioccipital bone (B in Fig. 2F), combined with an abnormally medial and caudal location of the inner ear (I in Fig. 2F). In the lower jaw

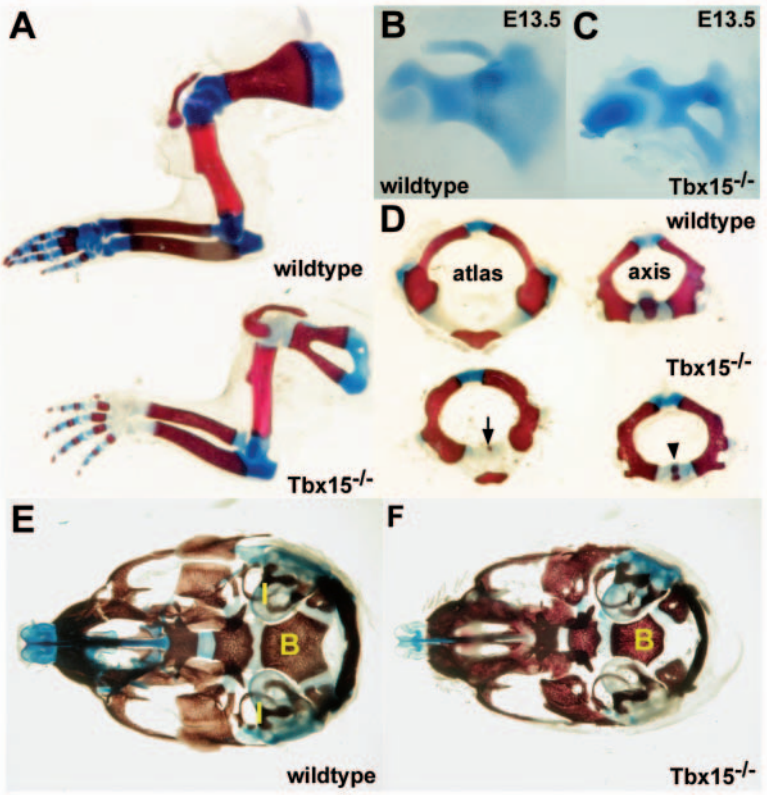

Fig. 2. Skeletal abnormalities of *Tbx15* mutants. Alcian Blue and Alizarin Red staining of newborn and E13.5 wild-type and *Tbx15* mutants. (A) Newborn *Tbx15* mutants have a foramen in the blade of the scapula and the humerus is shorter than in wild type. (B,C) Alcian Blue staining of E13.5 wild-type (B) and *Tbx15* mutant (C) shoulder girdle. At this stage the phenotype is already present. (D) Abnormalities of the caudal posterior aspect of vertebrae in newborn *Tbx15* mutants. Arrow indicates ectopic cartilage in the atlas of *Tbx15* mutant; arrowhead indicates the place were the dens of the axis is missing. (E,F) Cranial base of a newborn wild-type (E) and $Tbx15^{-/-}$ (F) skull. The *Tbx15* mutant skull is shorter and narrower than the wild type, and the basioccipital bone (B) is narrow when compared with wild type; also the inner ear (I) has an abnormal medial and caudal position.

of *Tbx15*$^{-/-}$, the dentaries are also shorter, with a short angular process (not shown).

The most characteristic defect in *Tbx15*$^{-/-}$ mice is the scapular foramen (Fig. 2A-C). The mutant's scapula is somewhat reduced in size compared with wild type and is more posteriorly and ventrally positioned. The scapular phenotype was already clearly visible at E13.5 (Fig. 2B,C), and at E12.5 was foreshadowed by an abnormal shape of the corresponding mesenchymal condensation. In addition, at E16.5 the acromion is reduced (black arrowhead in Fig. 3B).

Other parts of the skeleton do not show clear defects. In sharp contrast to the shoulder region, and in spite of very similar *Tbx15* expression in both fore- and hindlimb bud regions (Agulnik et al., 1998) (Fig. 1), the pelvic girdle is normal (Fig. 4E). In contrast to Curry, we did not observe a significant generalized reduction in bone size. Differences in genetic background and/or the fact that that author studied a different allele of *Tbx15* are likely to explain the weak expression of the phenotype in the animals in our study. The 100% penetrance of the scapular foramen emphasizes its significance and rules out the possibility that it is caused by merely a broad skeletogenic deficiency.

Tbx15 and *Gli3* act synergistically during shoulder girdle development

Extra toes (*Xt*^{J}) mutants have a disrupted *Gli3* gene (Schimmang et al., 1992; Hui and Joyner, 1993) and homozygosity of this mutation leads to a malformed shoulder girdle. Depending on genetic background, *Gli3* homozygotes may contain a foramen in the scapular blade (Johnson, 1967; Hui and Joyner, 1993), thus resembling the *droopy ear* phenotype. If this similarity resulted from *Gli3* and *Tbx15* functioning in the same pathway(s) during shoulder formation, one would expect little exacerbation of the phenotype in double mutants. To investigate this, we generated *Gli3*$^{-/-}$/*Tbx15*$^{-/-}$ homozygous compound mutants and compared the phenotypes of single and double mutants.

Skeletal staining of E16.5 fetuses showed a severe reduction of the scapular blade in *Gli3*$^{-/-}$/*Tbx15*$^{-/-}$mutants (Fig. 3F) when compared to either single mutant (Fig. 3B,C). Only the most anterior part of the scapular blade (supraspinatus fossa) remained, as well as a small part of the edge of the blade. Furthermore, the acromion was more severely reduced (arrowhead in Fig. 3B,D,F), whereas the glenoid fossa (scapular head) was normal. This aggravated shoulder

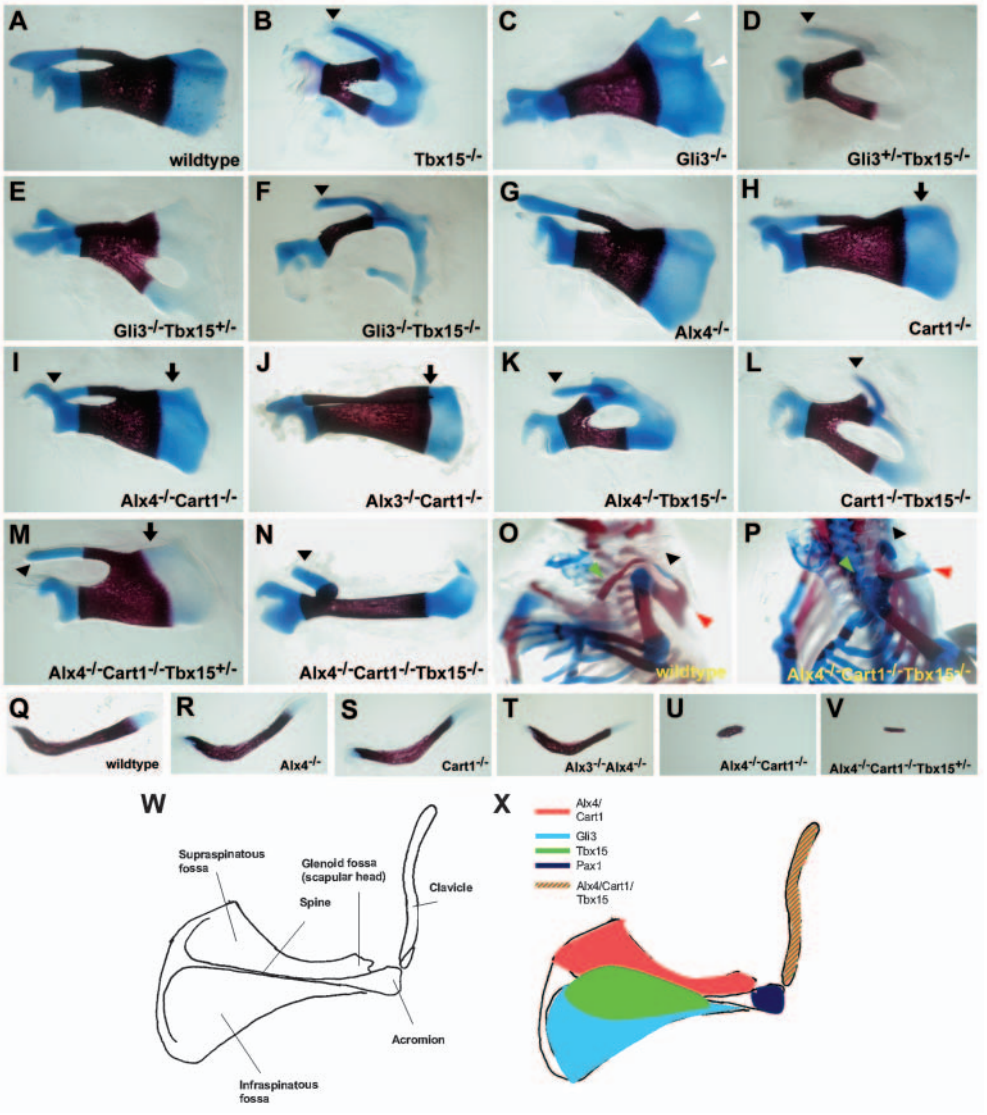

Fig. 3. The scapular blade is severely affected in *Tbx15*/*Gli3* and *Alx4*/*Cart1*/*Tbx15* compound mutants. (A-N) Skeletal staining of the shoulder girdle of E16.5 embryos. Black arrowheads (B,D,F,I,K-N) indicate the reduced acromion in *Tbx15*/*Gli3* and Alx4/*Cart1*/*Tbx15* mutants; white arrowheads (C) indicate the indentations in the scapular blade of *Gli3* mutants; black arrows (H-J,M) indicate the reduction of the anterior part of the scapular blade in *Alx3*/*Alx4*, *Alx4*/*Cart1* and *Alx4*/*Cart1*/*Tbx15* compound mutants. Note the severely reduced acromion and the remaining posterior part of the scapular blade in the *Alx4*$^{-/-}$*Cart1*$^{-/-}$*Tbx15*$^{-/-}$ mutant shoulder girdle (N). (O,P) Side view of the intact skeleton of wild-type (O) and *Alx4*$^{-/-}$/*Cart1*$^{-/-}$/*Tbx15*$^{-/-}$ (P) embryos at E16.5. Green arrowhead in O indicates the clavicle, which is missing in *Alx4*/*Cart1*/*Tbx15* mutants (green arrowhead in P). Red arrowhead indicates the scapula; black arrowhead indicates the acromion. (Q-V) Clavicles of *Alx3*/*Alx4*/*Cart1*/*Tbx15* compound mutants. The clavicle size is slightly reduced in *Alx3*/*Alx4* double mutants (T), but only a small remnant of the clavicle is visible in *Alx4*/*Cart1* (U) and *Alx4*$^{-/-}$*Cart1*$^{-/-}$*Tbx15*$^{+/-}$ mutants (V). (W) Schematic representation of the elements of the shoulder girdle. (X) Schematic representation of the distinct functions of *Alx4*/*Cart1* (red), *Gli3* (blue) and *Tbx15* (green) during shoulder girdle development. *Alx4*, *Cart1* and *Tbx15* (red/green) have functions during clavicle development.

phenotype is clearly dependent on gene dosage because the scapular foramen of *Gli3*$^{+/-}$/*Tbx15*$^{-/-}$ mutants is enlarged in comparison with *Tbx15*$^{-/-}$ single mutants (compare Fig. 3B and 3D). Although we never observed a scapular foramen in the *Gli3* mutants used in our study, the shoulder elements were broader than those in wild types, and contained indentations in the scapular blade (white arrowheads in Fig. 3C). In *Tbx15*$^{+/-}$/*Gli3*$^{-/-}$ mutants these malformations were enhanced, the scapular blade was still broader and a foramen in the scapula was now present (Fig. 3E).

In conclusion, the phenotypes of compound mutants suggest that *Tbx15* and *Gli3* act synergistically during shoulder girdle formation, representing at some level a degree of functional redundancy.

Functions of *Alx3*, *Alx4* and *Cart1* in limb girdle development

Previously, we, and others, have studied the roles of *Alx3*, *Alx4* and *Cart1*, with an emphasis on limb and craniofacial development. These three genes have strongly overlapping functions in limb and craniofacial development (Qu et al., 1999; Beverdam et al., 2001) (also A.B., unpublished). We reported severe truncation of the collar bone (clavicle) of *Alx3*/*Alx4* mutants, but not of either single mutant (Beverdam et al., 2001) (see Fig. 3T); otherwise these genes have not been linked to pectoral or pelvic girdle development.

Close inspection of the shoulder elements of *Cart1* mutants revealed a slight reduction of the anterior blade in this single mutant, although the acromion was normal (Fig. 3H). In *Alx4*/*Cart1* mutants (Fig. 3I,U), not only was the clavicle truncation much more severe than in *Alx3*/*Alx4* mutants, but also the scapular blade rostral from the spine was virtually absent, and the spine itself and the acromion was shortened (arrowhead in Fig. 3I). Analyses of various compound genotypes showed similarly affected phenotypes in all double homozygous mutants (Fig. 3I,J); however, it was clear that inactivation of *Cart1* had the most impact and that the impact of *Alx3* mutation was much less. In conclusion, *Cart1* has a major function in scapula formation that becomes clearly manifest only in the context of mutation(s) in *Alx4*, with which it shares an overlapping function.

In contrast to *Tbx15* mutants, and also not previously reported, the pelvic girdle of *Alx4*/*Cart1* double mutants is affected as well. Although *Alx3* and *Cart1* single mutants were normal (not shown), we noticed that *Alx4* mutants had a reduced pubic bone (arrowhead in Fig. 4B). However, the pubic bone was more severely affected in *Alx3*/*Alx4* and *Alx4*/*Cart1* compound mutants (Fig. 4C,D). Note that the ilium of the mutant was normal, and that the scapula and pubic bone serve non-analogous functions. Therefore, *Alx3*, *Alx4 and Cart1* have overlapping functions in the formation of elements of both the pectoral and pelvic girdle, but different structures are affected. By contrast, loss of function of, for example, *Emx2* and *Pbx1* affects the scapula and ilium in similar ways (Pellegrini et al., 2001; Selleri et al., 2001).

Genetic relationship between *Tbx15*, *Alx4* and *Gli3* mutants

We generated *Alx4*/*Cart1*/*Tbx15* mutant embryos to investigate possible genetic interactions in the way these genes pattern the shoulder girdle. Upon skeletal staining of *Alx4*/*Cart1*/*Tbx15* triple mutants at E16.5, a severe reduction of the scapular blade was observed (Fig. 3N). The only remnants of the scapula were the glenoid fossa (scapular head), a small fraction of the acromion (arrowhead in Fig. 3N) and the posterior part of the blade (the infraspinatus fossa). The clavicle was completely absent, as is shown in an intact skeleton (Fig. 3O,P).

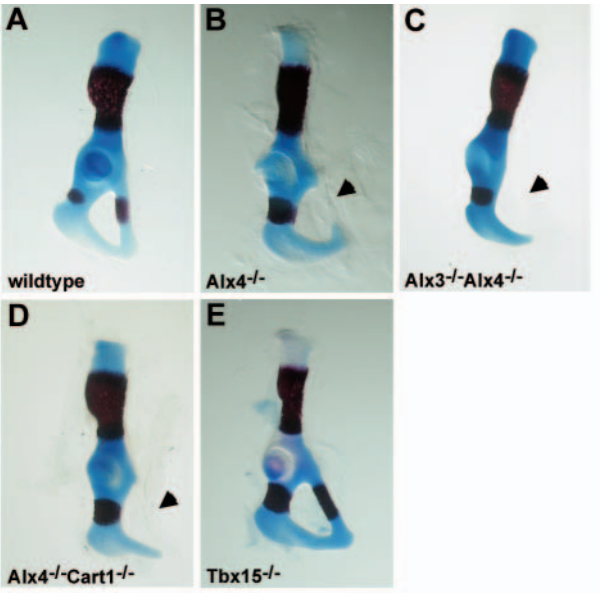

Fig. 4. Pelvic abnormalities in *Alx4* mutants. (A-E) Skeletal staining of pelvic girdles of E16.5 embryos. Black arrowhead indicates a reduction or absence of the pubic bone in *Alx4* (B), *Alx3*/*Alx4* (C), *Alx4*/*Cart1* (D) mutants, whereas the pelvic girdle in *Tbx15* mutants (E) was not affected.

The severity of the phenotype depends on gene dosage as shown by intermediate phenotypes in a *Tbx15*$^{+/-}$ background. For example, in *Cart1*/*Tbx15* compound mutants the hole in the scapula is larger than in *Tbx15* homozygotes (Fig. 3L), and in *Alx4*$^{-/-}$/*Cart1*$^{-/-}$/*Tbx15*$^{+/-}$ the spine was more reduced, the scapular blade was more severely malformed than in *Alx4*/*Cart1* mutants, and a tiny remnant of the clavicle was present (compare Fig. 3I and 3M, and Fig. 3U and 3V). These results demonstrate that *Tbx15* acts cooperatively with *Alx4* and *Cart1* in the development of the scapula. Comparing phenotypes of single and double mutants does not necessarily imply synergism between aristaless-related and T-box genes, as it appears that the defects are largely additive.

Similarly, we generated *Gli3*/*Tbx15* compound mutants. This not only allows the investigation of genetic interactions between these two genes, but also provides an opportunity to compare the impact on shoulder formation, of the *Alx4* and *Cart1* genes on the one hand and of the similarly expressed *Gli3* gene on the other. *Alx4*/*Cart1*/*Tbx15* triple mutants and *Gli3*/*Tbx15* compound mutants show strikingly contrasting phenotypes. By and large, whereas *Alx4*/*Cart1*/*Tbx15* homozygous triple mutants lacked the anterior part of the scapular blade, *Gli3*/*Tbx15* double mutants lacked the posterior part of the blade (compare Fig. 3F and 3N). Therefore, against the background of deficient *Tbx15* function, the different roles of *Alx4* and *Cart1*, when compared with *Gli3*, become more conspicuous.

Gene regulation in shoulder mutants

To begin to clarify the molecular pathways underlying shoulder girdle development in mammals, we studied the expression of genes that are functionally linked to this process in *Alx4*, *Cart1*, *Tbx15*, and *Gli3* single and compound mutants. First, we set out to study the expression patterns of *Tbx15*, *Alx4*, *Cart1* and *Gli3* in the mutants used in this study. *Alx4* has previously been reported to be downregulated in the limb buds of *Gli3* mutants; however, this concerns only the most distal part of the expression domain, which would therefore not be expected to be relevant for the phenotype of the scapula (Te Welscher et al., 2002) (see Fig. 1D,E). We observed that expression of *Tbx15* in *Alx4*, *Cart1* and *Gli3* mutant limb buds at E10.5 and E11.5 was not altered, and neither was expression of *Alx4* and *Gli3* in *Tbx15*$^{-/-}$ mutant limb buds at E10.5 (data not shown).

Emx2 has an essential role during shoulder development. It is normally expressed in the anterior-proximal region of the forelimb bud and at the base of the hindlimb bud. Its ablation leads to loss of both the scapula and the ilium (Pellegrini et al., 2001). Expression of *Emx2* was unaltered in *Alx4*/*Cart1* single and double mutants, and in *Tbx15*/*Gli3* single and double mutants (Fig. 1F-I), suggesting that *Emx2* acts in a parallel pathway or upstream of *Alx4*, *Cart1*, *Gli3* and *Tbx15*.

Pax1 has a well-documented function in shoulder formation (Timmons et al., 1994; Dietrich and Gruss, 1995). In addition to being a sclerotome marker, *Pax1* is normally expressed in mesenchyme in the anterior proximal part of the fore- and hindlimb bud (Timmons et al., 1994). We therefore studied *Pax1* expression in various mutants with an affected shoulder phenotype. Expression of *Pax1* was not altered in *Alx4* and *Cart1* single mutants at E10.5 (Fig. 5F,G). Strikingly, in *Alx4*$^{-/-}$/*Cart1*$^{-/-}$ the expression of *Pax1* in the limb bud was strongly reduced at the site of its normal expression (Fig. 5H) and was upregulated in the ventral body wall adjacent to the limb bud. Images from a different angle are required to demonstrate this shift: Fig. 5I-L show ventral aspects of the forelimb region of a wild type, an *Alx4*$^{+/-}$/*Cart1*$^{-/-}$ mutant and two *Alx4*$^{-/-}$/*Cart1*$^{-/-}$ mutants at E10.5. This clearly reveals a dose-dependent upregulation of *Pax1* in body wall mesenchyme. In situ hybridization on sections confirmed the downregulation at E10.5 (Fig. 5Q,R). At E11.5, the Pax1 expression pattern is still clearly abnormal in mutant limb buds, as shown for both fore- and hind limb (compare Fig. 5M,O to 5N,P, respectively). In *Tbx15*$^{-/-}$ embryos at E10.5, a weaker yet still significant downregulation of antero-proximal *Pax1* expression was seen (Fig. 5B), whereas in *Gli3*$^{-/-}$ embryos this effect was somewhat stronger (compare Fig. 5B and C). In *Gli3*/*Tbx15* double mutants, *Pax1* expression was slightly lower than in *Gli3* mutants. (Fig. 5D). However, a shift like the one seen in *Alx4*/*Cart1* mutants was, at most, weakly present in *Tbx15* embryos and was absent from *Gli3* embryos.

To investigate whether and to what extent altered apoptosis might contribute to the altered *Pax1* expression domain, we compared Nile Blue stainings of whole-mount wild-type and Alx4$^{-/-}$/Cart1$^{-/-}$ E10.5 embryos, and cleaved Caspase-3 antibody stainings of sectioned embryos, but no significant differences were noted (data not shown). Proliferation, as detected using an antibody against the phosphorylated form of Histone 3, did not show significant differences between wild-type and mutant embryos either. In view of the implied non-overlapping expression patterns of the genes, another explanation for the aberrant expression of *Pax1* would be that in *Alx4*/*Cart1*, and perhaps in *Tbx15*, mutants, positional cues have been disrupted, which may interfere with the normal recruitment of cells homing for the scapula region, eventually leading to malformations of skeletal elements of the shoulder girdle. To further investigate this, we analyzed the expression of *Scleraxis* and *Pax3*.

Although *Pax1* is considered to be a marker of the chondrocyte lineage, *Pax3* is thought to mark, in the context of limb development, the myogenic lineage. Recently, the syndetome was identified as a fourth component of the somite, consisting of tendon progenitors that are distinguished by expression of *Scleraxis* (*Scx*) as a marker (Brent et al., 2003). We compared the expression of *Pax3* and *Scx* in limb buds of E10.75 *Alx4*/*Cart1* mutant and wild-type embryos. From the whole-mount in situ hybridization experiment shown in Fig. 5V, it can be seen that *Pax3* expression is shifted towards the antero-proximal region of the limb bud in a region where *Pax1* is downregulated. In addition, hybridization of sections of *Alx4*/*Cart1* mutants with *Pax3* demonstrated that *Pax3* expression in the body wall (marking myotonic progenitors from the dermomyotome and heading for the limb) is abnormally located in mesenchyme, just adjacent to surface ectoderm (Fig. 5S,T). *Scx* expression was changed to a lesser degree, but appeared to be elevated in the antero-proximal region of the limb bud in the *Alx4*/*Cart1* mutant (green arrowhead in Fig. 5X). Fig. 5Y summarizes these results schematically. We conclude that different types of migrating cells that are bound to contribute to the pectoral girdle are disorganized in shoulder mutants at an embryonic stage prior to visible anatomical aberrations. Possibly it is cell migration itself that is affected, but alternatively a transformation of cells involved may take place. By contrast, no ectopic expression of *Pax3* or *Scx* was seen in *Tbx15* mutants, or in *Tbx15*/*Gli3* mutants (data not shown).

Discussion

The developmental pathways responsible for patterning of the skeletal elements in the mammalian pectoral and pelvic girdles have remained rather obscure. Extrapolation of experimental results obtained in grafting experiments in avian species suggests that the scapula derives from a set of dermomyotomes, whereas other elements would have a somatopleural origin. The paradoxical origin of an endochondral skeletal element like the scapula from dermomytome has led to speculation that it arose during evolution by the ossification of muscles (Burke, 2000; Huang et al., 2000). If this is a correct representation of the ontogeny of these elements, it is understandable that the mechanisms that underlie their formation differ from those of the well-known signaling centers that shape the vertebrate. Indeed, many mutations that affect limb formation have little or no impact on the pectoral and pelvic girdles.

In this study, we have explored the genetic interactions of a number of genes that are implicated in formation of the pectoral (and to a lesser extent pelvic) girdle skeleton. The study of genotype-phenotype relations in complex compound mutants allows genetic relationships between genes to be determined, and the recognition of important gene

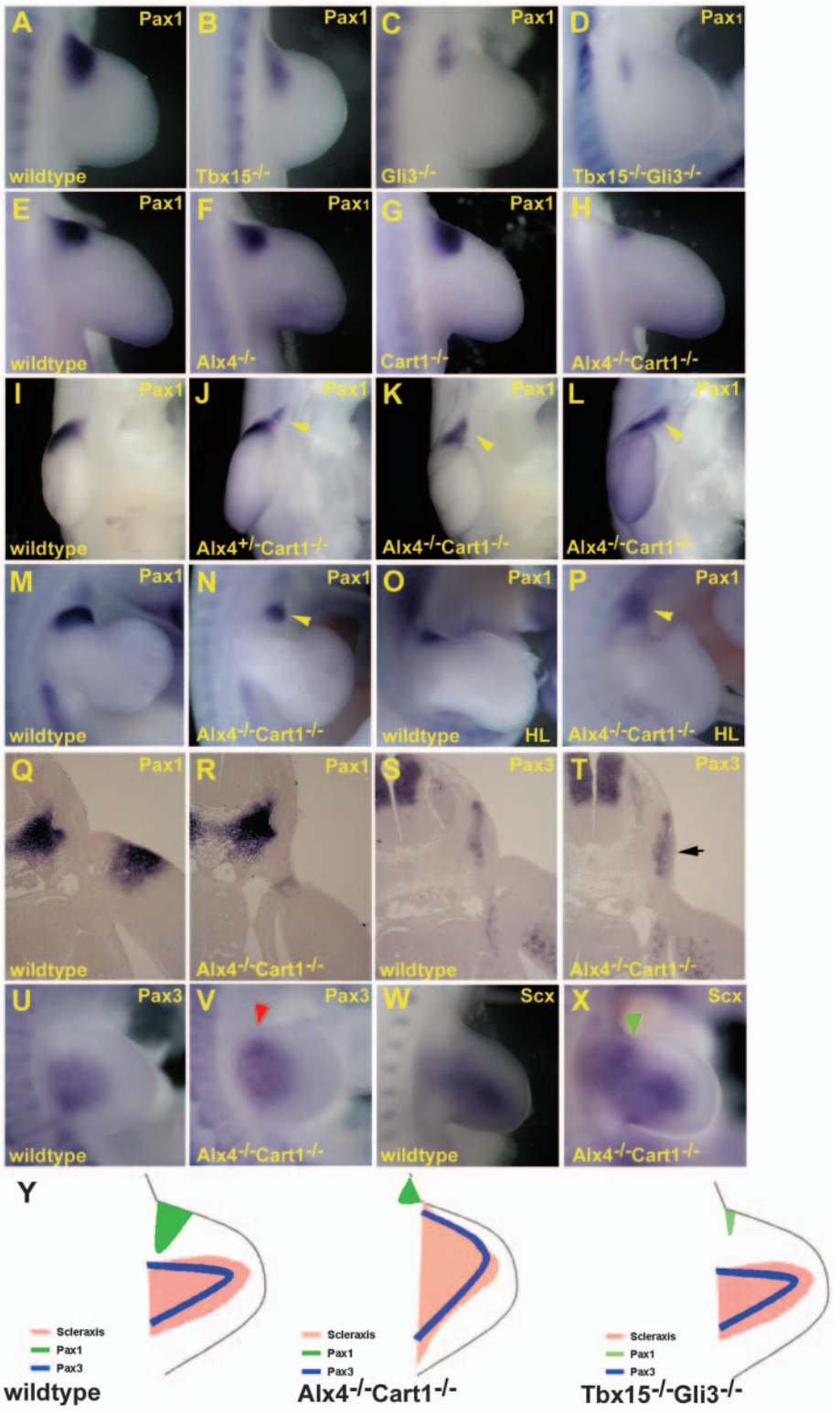

Fig. 5. Gene regulation in *Alx4*, *Cart1*, *Gli3* and *Tbx15* compound mutants. (A-D) *Pax1* expression in E10.5 wild-type (A), *Tbx15*$^{-/-}$ (B), *Gli3*$^{-/-}$ (C) and *Tbx15*/*Gli3* double mutant (D) forelimb buds. Note the downregulation of *Pax1* expression in the mutants. (E-L) *Pax1* expression in E10.75 wild-type (E,I), *Alx4*$^{-/-}$ (F), *Cart1*$^{-/-}$ (G), *Alx4*$^{+/-}$/*Cart1*$^{-/-}$ (J) and *Alx4*$^{-/-}$/*Cart1*$^{-/-}$ (H,K,L) forelimb buds. (E-H) Dorsal views of the limb buds. Note the downregulation of *Pax1* in *Alx4*/*Cart1* compound mutants (H). (I-L) Ventral view of the limb buds. Yellow arrowhead indicates the shift of *Pax1* expression in *Alx4*$^{+/-}$/*Cart1*$^{-/-}$ (J) and *Alx4*$^{-/-}$/*Cart1*$^{-/-}$ (K,L) mutants. (M-P) *Pax1* expression in wild-type (M,O) and *Alx4*/*Cart1* mutant (N,P) fore- and hindlimb (HL) buds at E11.5. Yellow arrowhead (N,P) indicates the shift of *Pax1* expression. (Q-T) In situ hybridization on serial transversal sections at E10.5 of wild-type (Q,S) and *Alx4*/*Cart1* mutant (R,T) embryos. (Q,R) *Pax1* expression is downregulated in *Alx4*/*Cart1* mutants. (S,T) *Pax3* is abnormally expressed in the mesenchyme just adjacent to the surface ectoderm in *Alx4*/*Cart1* mutants (black arrow in T). (U,V) Whole-mount in situ hybridization with *Pax3* probe of E10.5 wild-type (U) and *Alx4*/*Cart1* mutant (V) limb buds. Red arrowhead (V) indicates *Pax3* expression that is shifted towards the antero-proximal region of the limb bud. (W,X) Expression of *Scleraxis* (*Scx*) in E10.5 wild-type (W) and *Alx4*/*Cart1* mutant (X) limb buds. Green arrowhead (X) indiactes the shift of *Scx* expression in the *Alx4*/*Cart1* mutant. (Y) Schematic representation of the expression patterns of *Pax1*, *Pax3* and *Scleraxis* in wild type, and in *Alx4*/*Cart1* and *Tbx15*/*Gli3* compound mutants.

functions otherwise masked because of redundancy.

Aristaless-related genes

We show that *Cart1* and *Alx4* single mutants have slight, not previously reported, defects in skeletal elements of the pectoral and pelvic girdle, respectively, that become more severe in double mutants carrying additional mutations in either one of the three redundant genes *Alx3*, *Alx4* and *Cart1*. Whereas *Emx2* appears to be essential for the formation of structures of both girdles (scapula and ilium) that look superficially similar (Pellegrini et al., 2001), Alx4/Cart1 mutants, as well as *Tbx15* mutants, have very different phenotypes in the shoulder and pelvis. There is no sound basis for describing both girdles in terms of homology; clearly evolution of the girdles has evolved separately and under different species-specific constraints. During evolution, the aristaless-related genes may have been recruited for different functions in development of both types of girdle. Any speculation on such topics is rather futile in the absence of both mutants from appropriate different species and expression data from extinct ancestors. The pubic bone is also affected in mutants for the aristaless-related genes *Prx1* and *Prx2* (Ten Berge et al., 1998b), which have overlapping but broader expression patterns and are generally linked to different phenotypes.

The prevailing function of *Cart1* that emerges from comparing compound mutants involving *Alx3*, *Alx4* and *Cart1* is also unexpected because *Cart1* is expressed only at low levels in mesoderm of the limb buds and flank (Zhao et al., 1994; Beverdam and Meijlink, 2001). This paradox was previously noted for the polydactyly in *Alx4*/*Cart1* double mutants (Qu et al., 1999).

Distinct functions of *Gli3* and *Alx4* revealed in *Tbx15* double mutants

The striking scapular foramen characteristic of *Tbx15* mutants shows that this gene is essential for appropriate shoulder formation. *Gli3* mutants kept in certain genetic backgrounds have a similar foramen. The combined deficiency of these two genes, however, resulted in a unique phenotype in which the anterior part of the scapula remained, leaving a structure that resembled a typical long bone (e.g. Fig. 3F). Such an element also resulted from *Alx4*/*Cart1*/*Tbx15* triple homozygous mutants (Fig. 3N), but in this case through ablation of the anterior part of the scapula. These contrasting phenotypes reveal complementary functions of *Gli3* and *Alx4*/*Cart1*, linking *Gli3* to the posterior part of the scapular blade (infraspinatus fossa), and *Alx4* and *Cart1* to the anterior part (supraspinatus fossa), as depicted in the schematic representation in Fig. 3W,X. Interestingly, *Alx4* and *Gli3* have strongly overlapping expression patterns in the anterior mesoderm of the limb bud. Both genes are also examples of genes whose functions are linked to formation of both the shoulder and distal limb elements. Furthermore, *Alx4* expression is partly dependent on *Gli3* function (see Fig. 1D,E) (see also Te Welscher et al., 2002), but the region of *Alx4* downregulation in *Gli3* mutants is not likely to be relevant for shoulder formation (e.g. Vargesson et al., 1997). Presumably *Alx4*-associated phenotypes, including radial/tibial dysplasia and polydactyly, relate to different aspects of its expression pattern, and it is possible that the expression that disappears in *Gli3* mutants corresponds to the zeugopodal and autopodal functions.

Defects of the clavicle

In contrast to the scapula, the clavicle arises through intramembranous rather than endochondral ossification. It evolved in primitive fish as a skeletal element at the base of the skull (see McGonnell et al., 1998), and, in mammals, is the only membranous bone outside of the skull. *Alx4* and related genes have a function in shaping the neural crest-derived craniofacial skeleton, and we can therefore not exclude that the clavicle phenotypes we describe should be seen in that context. Nevertheless, a degree of redundancy can be seen between *Tbx15* and *Alx4*/*Cart1*, even leading to complete suppression of the clavicle in the triple homozygous mutant. We therefore favor the notion that a similar disorganization locally in the shoulder girdle that also causes the scapular defect is the basis of the interference with clavicle formation.

Pax1 and *Pax3* dysregulation in shoulder mutants

In the differentiating somite, the *Pax1* gene is a sclerotomal marker. In the context of formation of the scapula, however, which is of dermomyotomal derivation, it is primarily considered to be a chondrocyte marker. *Pax1* is linked to shoulder formation by the phenotype of *undulated* and other mutant alleles (Balling et al., 1988; Deutsch et al., 1988). *Pax1* mutants lack part of the spine and the cartilaginous acromion. In addition, *Pax1* is abnormally expressed in a number of shoulder mutants. Pellegrini showed that *Pax1* was upregulated and shifted dorsally in *Emx2* mutants that have totally lost the scapula (Pellegrini et al., 2001). By contrast, we demonstrate a downregulation and ventral shift of *Pax1* expression associated with the scapula truncation in *Alx4*/*Cart1* mutants, whereas loss of *Gli3* or *Tbx15* function leads to a similar downregulation, but without the ventral upregulation. *Pax1* is inhibited by the application of beads containing BMP4 in chick limb buds, which is accompanied by scapula defects (Hofmann et al., 1998); however, it is induced by Sonic hedgehog (SHH) application (Laufer et al., 1994). At later stages, *Shh* is even upregulated in the anterior limb bud of *Alx4* mutants (Chan et al., 1995). At E10.5, both *Bmp4* and *Shh* were normally expressed in the limb regions of *Alx4*/*Cart1* mutant embryos (data not shown). This suggests that these signaling pathways are not downstream of *Alx4* and *Cart1* in the mechanism leading to *Pax1* deregulation in mutants. Intriguingly, *Tbx15* and *Pax1* have complementary rather than overlapping expression patterns (Fig. 1A,C), basically ruling out direct interaction. It should be noted that *Tbx15*, *Alx4* (S.K., unpublished) and *Cart1* (Ten Berge et al., 1998a) are not expressed in the dermomytome, which is in contrast with the high dermomyotomal expression of *Gli3* reported by McDermott and colleagues (McDermott et al., 2005). It therefore remains possible that *Pax1* downregulation in *Gli3* mutants is a direct consequence of interaction between these genes, but the effect on *Pax1* expression seen in *Alx4*/*Cart1* mutants suggests a model in which *Pax1* deregulation reflects the disturbance of positional cues that guide cells destined to contribute to the shoulder. This would modify the view of *Pax1* as a mere marker of cartilage/bone precursors, although the affected morphology of the acromion seen in most of the mutants studied here may be directly related to the loss of *Pax1* in the acromioclavicular region where it is normally expressed. However, ectopic expression of *Pax1* does not lead to ectopic cartilage elements, possibly due to a lack of permissiveness in its abnormal area of expression. *Emx2* marks the prospective scapular blade region (Pellegrini et al., 2001; Pröls et al., 2004). The apparently normal *Emx2* expression in all mutants studied shows that the altered *Pax1* expression does not merely reflect the downregulation of markers for progenitors of structures that are affected.

Only recently has it fully emerged how genes specifically expressed in different somite compartments mark cells that migrate to the limb to form corresponding tissues. This process must depend on positional cues and its disruption is expected to be reflected in the expression of these markers. We therefore consider the shift in expression of *Pax3*, and to a lesser extent *Scx*, to support a model involving the disruption of positional signals, as suggested above. It should be noticed that the changes in expression of *Pax1*, *Pax3* and *Scx* are seen in regions of embryos at a stage when anatomical or histological aberrations are not yet detectable, strongly suggesting that this dysregulation is a part of the mechanism that leads to the eventual skeletal defects. It remains to be seen whether it is the process of migration that is disturbed or whether some type of transformation or abnormal differentiation results in the shoulder malformations. The latter possibility is not supported

by analyses of muscle tissue in *Alx4*/*Cart1* mutants, as we noted only loss of muscle tissue, in particular affecting the supraspinatus muscle (not shown). *de* mutant embryos also have reduced muscle tissue (Curry, 1959; Singh et al., 2005). Huang et al. have suggested an essential causal link between the downregulation of *Pax3* in a subset of hypaxial dermomyotomes and the potential of this tissue to differentiate into cartilage (and to contribute to scapula or ilium) (Huang et al., 2000). In this respect, it is interesting that overexpression of the modulator of Wnt-signaling Carboxypeptidase Z in the dermomytome of chick embryos leads to scapular defects, as well as ectopic *Pax3* expression (Moeller et al., 2003).

Results from grafting studies in chick embryos point to the importance of signals from the ectoderm to the underlying mesoderm, and the possible implication of FGF signaling (Ehehalt et al., 2004; Pröls et al., 2004). In *Alx4* mutants at E10.5, FGF4 is ectopically expressed in anterior limb bud ectoderm (Chan et al., 1995). Identifying the exact nature of the signaling cascade underlying scapula formation is a major challenge and may require combining genetics with the manipulation of embryo explants.

We are very grateful to Benoît de Crombrugghe for making the *Cart1* mice available. We also thank Eduardo Boncinelli, Uwe Deutsch, Eric N. Olson and Rolf Zeller for probes, Jeroen Korving for histology, and Jacqueline Deschamps for reading the manuscript. S.K. is supported by the Netherlands Research Organization NWO (grant 810.68.013 to F.M.).

References

Agulnik, S. I., Papaioannou, V. E. and Silver, L. M. (1998). Cloning, mapping, and expression analysis of TBX15, a new member of the T-Box gene family. *Genomics* **51**, 68-75.

Ahn, D. G., Kourakis, M. J., Rohde, L. A., Silver, L. M. and Ho, R. K. (2002). T-box gene tbx5 is essential for formation of the pectoral limb bud. *Nature* **417**, 754-758.

Aubin, J., Lemieux, M., Tremblay, M., Behringer, R. R. and Jeannotte, L. (1998). Transcriptional interferences at the Hoxa4/Hoxa5 locus: importance of correct Hoxa5 expression for the proper specification of the axial skeleton. *Dev. Dyn.* **212**, 141-156.

Balling, R., Deutsch, U. and Gruss, P. (1988). undulated, a mutation affecting the development of the mouse skeleton, has a point mutation in the paired box of Pax 1. *Cell* **55**, 531-535.

Begemann, G., Gibert, Y., Meyer, A. and Ingham, P. W. (2002). Cloning of zebrafish T-box genes tbx15 and tbx18 and their expression during embryonic development. *Mech. Dev.* **114**, 137-141.

Beverdam, A. and Meijlink, F. (2001). Expression patterns of group-I aristaless-related genes during craniofacial and limb development. *Mech. Dev.* **107**, 163-167.

Beverdam, A., Brouwer, A., Reijnen, M., Korving, J. and Meijlink, F. (2001). Severe nasal clefting and abnormal embryonic apoptosis in Alx3/Alx4 double mutant mice. *Development* **128**, 3975-3986.

Brent, A. E., Schweitzer, R. and Tabin, C. J. (2003). A somitic compartment of tendon progenitors. *Cell* **113**, 235-248.

Burke, A. C. (2000). Hox genes and the global patterning of the somitic mesoderm. *Curr. Top. Dev. Biol.* **47**, 155-181.

Candille, S. I., Raamsdonk, C. D., Chen, C., Kuijper, S., Chen-Tsai, Y., Russ, A., Meijlink, F. and Barsh, G. S. (2004). Dorsoventral patterning of the mouse coat by tbx15. *PLoS. Biol.* **2**, E3.

Chan, D. C., Laufer, E., Tabin, C. and Leder, P. (1995). Polydactylous limbs in Strong's Luxoid mice result from ectopic polarizing activity. *Development* **121**, 1971-1978.

Core, N., Bel, S., Gaunt, S. J., Aurrand-Lions, M., Pearce, J., Fisher, A. and Djabali, M. (1997). Altered cellular proliferation and mesoderm patterning in Polycomb-M33-deficient mice. *Development* **124**, 721-729.

Cserjesi, P., Brown, D., Ligon, K. L., Lyons, G. E., Copeland, N. G., Gilbert, D. J., Jenkins, N. A. and Olson, E. N. (1995). Scleraxis: A basic helix-loop-helix protein that prefigures skeletal formation during mouse embryogenesis. *Development* **121**, 1099-1110.

Curry, G. (1959). Genetical and developmental studies on droopy-eared mice. *J. Embryol. Exp. Morphol.* **7**, 39-65.

Deutsch, U., Dressler, G. R. and Gruss, P. (1988). Pax 1, a member of a paired box homologous murine gene family, is expressed in segmented structures during development. *Cell* **53**, 617-625.

Dietrich, S. and Gruss, P. (1995). undulated phenotypes suggest a role of Pax-1 for the development of vertebral and extravertebral structures. *Dev. Biol.* **167**, 529-548.

Ehehalt, F., Wang, B., Christ, B., Patel, K. and Huang, R. (2004). Intrinsic cartilage-forming potential of dermomyotomal cells requires ectodermal signals for the development of the scapula blade. *Anat. Embryol. (Berl)* **208**, 431-437.

Goulding, M. D., Chalepakis, G., Deutsch, U., Erselius, J. R. and Gruss, P. (1991). Pax-3, a novel murine DNA binding protein expressed during early neurogenesis. *EMBO J.* **10**, 1135-1147.

Gregorieff, A., Grosschedl, R. and Clevers, H. (2004). Hindgut defects and transformation of the gastro-intestinal tract in Tcf4(–/–)/Tcf1(–/–) embryos. *EMBO J.* **23**, 1825-1833.

Hofmann, C., Drossopoulou, G., McMahon, A., Balling, R. and Tickle, C. (1998). Inhibitory action of BMPs on Pax1 expression and on shoulder girdle formation during limb development. *Dev. Dyn.* **213**, 199-206.

Huang, R., Zhi, Q., Patel, K., Wilting, J. and Christ, B. (2000). Dual origin and segmental organisation of the avian scapula. *Development* **127**, 3789-3794.

Hui, C. C. and Joyner, A. L. (1993). A mouse model of greig cephalopolysyndactyly syndrome: the extra-toesJ mutation contains an intragenic deletion of the Gli3 gene. *Nat. Genet.* **3**, 241-246.

Johnson, D. R. (1967). Extra-toes: anew mutant gene causing multiple abnormalities in the mouse. *J. Embryol. Exp. Morphol.* **17**, 543-581.

Laufer, E., Nelson, C. E., Johnson, R. L., Morgan, B. A. and Tabin, C. (1994). Sonic hedgehog and Fgf-4 act through a signaling cascade and feedback loop to integrate growth and patterning of the developing limb bud. *Cell* **79**, 993-1003.

Leussink, B., Brouwer, A., el Khattabi, M., Poelmann, R. E., Gittenberger-De Groot, A. C. and Meijlink, F. (1995). Expression patterns of the paired-related homeobox genes MHox/Prx1 and S8/Prx2 suggest roles in development of the heart and the forebrain. *Mech. Dev.* **52**, 51-64.

McGonnell, I. M., Clarke, J. D. W. and Tickle, C. (1998). Fate map of the developing chick face: analysis of expansion of facial primordia and establishment of the primary palate. *Dev. Dyn.* **212**, 102-118.

McDermott, A., Gustafsson, M., Elsam, T., Hui, C. C., Emerson, C. P., Jr and Borycki, A. G. (2005). Gli2 and Gli3 have redundant and context-dependent function in skeletal muscle formation. *Development* **132**, 345-357.

Meijlink, F., Kuijper, S., Brouwer, A. and Kroon, C. (2003). Prx, Alx and Shox genes in craniofacial and appendicular development. In *Murine Homeobox Gene Control of Embryonic Patterning and Organogenesis* (*Advances in Developmental Biology and Biochemistry*), Vol. 13 (ed. T. Lufkin), pp. 133-153. Amsterdam: Elsevier.

Moeller, C., Swindell, E. C., Kispert, A. and Eichele, G. (2003). Carboxypeptidase Z (CPZ) modulates Wnt signaling and regulates the development of skeletal elements in the chicken. *Development* **130**, 5103-5111.

Ng, J. K., Kawakami, Y., Buscher, D., Raya, A., Itoh, T., Koth, C. M., Rodriguez, E. C., Rodriguez-Leon, J., Garrity, D. M., Fishman, M. C. et al. (2002). The limb identity gene Tbx5 promotes limb initiation by interacting with Wnt2b and Fgf10. *Development* **129**, 5161-5170.

Niswander, L. (2003). Pattern formation: old models out on a limb. *Nat. Rev. Genet.* **4**, 133-143.

Pellegrini, M., Pantano, S., Fumi, M. P., Lucchini, F. and Forabosco, A. (2001). Agenesis of the scapula in Emx2 homozygous mutants. *Dev. Biol.* **232**, 149-156.

Pröls, F., Ehehalt, F., Rodriguez-Niedenfuhr, M., He, L., Huang, R. and Christ, B. (2004). The role of Emx2 during scapula formation. *Dev. Biol.* **275**, 315-324.

Qu, S. M., Tucker, S. C., Zhao, Q., De Crombrugghe, B. and Wisdom, R. (1999). Physical and genetic interactions between Alx4 and Cart1. *Development* **126**, 359-369.

Rallis, C., Bruneau, B. G., Del Buono, J., Seidman, C. E., Seidman, J. G., Nissim, S., Tabin, C. J. and Logan, M. P. (2003). Tbx5 is required for forelimb bud formation and continued outgrowth. *Development* **130**, 2741-2751.

Schimmang, T., Lemaistre, M., Vortkamp, A. and Ruther, U. (1992). Expression of the zinc finger gene Gli3 is affected in the morphogenetic mouse mutant extra-toes (Xt). *Development* **116**, 799-804.

Selleri, L., Depew, M. J., Jacobs, Y., Chanda, S. K., Tsang, K. Y., Cheah, K. S., Rubenstein, J. L., O'Gorman, S. and Cleary, M. L. (2001). Requirement for Pbx1 in skeletal patterning and programming chondrocyte proliferation and differentiation. *Development* **128**, 3543-3557.

Simeone, A., Acampora, D., Gulisano, M., Stornaiuolo, A. and Boncinelli, E. (1992). Nested expression domains of four homeobox genes in developing rostral brain. *Nature* **358**, 687-690.

Singh, M. K., Petry, M., Haenig, B., Lescher, B., Leitges, M. and Kispert, A. (2005). The T-box transcription factor Tbx15 is required for skeletal development. *Mech. Dev.* **122**, 131-144.

Takeuchi, J. K., Koshiba-Takeuchi, K., Suzuki, T., Kamimura, M., Ogura, K. and Ogura, T. (2003). Tbx5 and Tbx4 trigger limb initiation through activation of the Wnt/Fgf signaling cascade. *Development* **130**, 2729-2739.

Te Welscher, P., Fernandez-Teran, M., Ros, M. A. and Zeller, R. (2002). Mutual genetic antagonism involving GLI3 and dHAND prepatterns the vertebrate limb bud mesenchyme prior to SHH signaling. *Genes Dev.* **16**, 421-426.

Ten Berge, D., Brouwer, A., el Bahi, S., Guenet, J. L., Robert, B. and Meijlink, F. (1998a). Mouse Alx3: an aristaless-like homeobox gene expressed during embryogenesis in ectomesenchyme and lateral plate mesoderm. *Dev. Biol.* **199**, 11-25.

Ten Berge, D., Brouwer, A., Korving, J., Martin, J. F. and Meijlink, F. (1998b). Prx1 and Prx2 in skeletogenesis: roles in the craniofacial region, inner ear and limbs. *Development* **125**, 3831-3842.

Timmons, P. M., Wallin, J., Rigby, P. W. and Balling, R. (1994). Expression and function of Pax 1 during development of the pectoral girdle. *Development* **120**, 2773-2785.

Vargesson, N., Clarke, J. D. W., Vincent, K., Coles, C., Wolpert, L. and Tickle, C. (1997). Cell fate in the chick limb bud and relationship to gene expression. *Development* **124**, 1909-1918.

Zhao, G. Q., Eberspaecher, H., Seldin, M. F. and De Crombrugghe, B. (1994). The gene for the homeodomain-containing protein Cart-1 is expressed in cells that have a chondrogenic potential during embryonic development. *Mech. Dev.* **48**, 245-254.

Zhao, Q., Behringer, R. R. and De Crombrugghe, B. (1996). Prenatal folic acid treatment suppresses acrania and meroanencephaly in mice mutant for the Cart1 homeobox gene. *Nat. Genet.* **13**, 275-283.